

# High Performance Composites with Active Stiffness Control

Charnwit Tridech,<sup>†</sup> Henry A. Maples,<sup>†</sup> Paul Robinson,<sup>‡</sup> and Alexander Bismarck<sup>\*,†,§</sup>

<sup>†</sup>Polymer & Composite Engineering (PaCE) Group, Department of Chemical Engineering, Imperial College London, South Kensington Campus, London, SW7 2AZ, UK

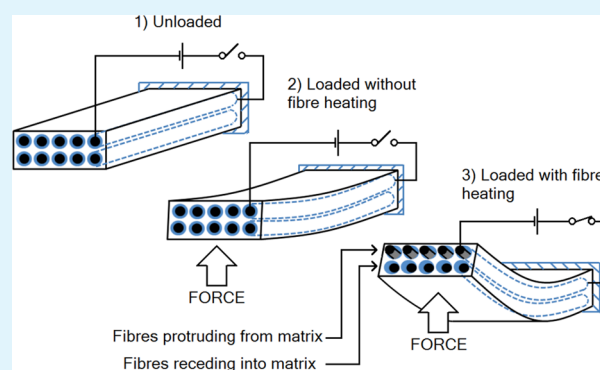
<sup>‡</sup>The Composite Centre, Department of Aeronautics, Imperial College London, South Kensington Campus, London, SW7 2AZ, UK

<sup>§</sup>Polymer and Composite Engineering (PaCE) Group, Institute of Materials Chemistry and Research, Faculty of Chemistry, University of Vienna, Währinger Straße 42, A-1090 Vienna, Austria

## Supporting Information

**ABSTRACT:** High performance carbon fiber reinforced composites with controllable stiffness could revolutionize the use of composite materials in structural applications. Here we describe a structural material, which has a stiffness that can be actively controlled on demand. Such a material could have applications in morphing wings or deployable structures. A carbon fiber reinforced–epoxy composite is described that can undergo an 88% reduction in flexural stiffness at elevated temperatures and fully recover when cooled, with no discernible damage or loss in properties. Once the stiffness has been reduced, the required deformations can be achieved at much lower actuation forces. For this proof-of-concept study a thin polyacrylamide (PAAm) layer was electrocoated onto carbon fibers that were then embedded into an epoxy matrix via resin infusion. Heating the PAAm coating above its glass transition temperature caused it to soften and allowed the fibers to slide within the matrix. To produce the stiffness change the carbon fibers were used as resistance heating elements by passing a current through them. When the PAAm coating had softened, the ability of the interphase to transfer load to the fibers was significantly reduced, greatly lowering the flexural stiffness of the composite. By changing the moisture content in PAAm fiber coating, the temperature at which the PAAm softens and the composites undergo a reduction in stiffness can be tuned.

**KEYWORDS:** morphing, stiffness control, composite, carbon fibers, epoxy



## 1. INTRODUCTION

Composite materials with controllable stiffness could be used in applications such as morphing skins<sup>1,2</sup> and wings,<sup>3,4</sup> deployable structures,<sup>5</sup> vibration control (damping),<sup>6</sup> and customized shape tailoring.<sup>5</sup> For morphing aerostructures a stiff skin material is required that can be deformed on demand with acceptable actuation forces.<sup>3</sup> In previous studies materials such as elastomers were selected as morphing skins;<sup>7</sup> however, unlike aerospace materials they cannot withstand high aerodynamic loads.<sup>8</sup> Variable stiffness materials have previously been developed for morphing applications.<sup>9–11</sup> Henry and McKnight developed a composite consisting of a Shape Memory Polymer (SMP) reinforced with discontinuous steel.<sup>12</sup> The matrix was softened above its glass transition temperature ( $T_g$ ), and this reduced the stiffness of the composite. A problem with designs such as these is that reductions in stiffness can only occur when the entire matrix has softened. Deforming these composites at elevated temperature could therefore lead to permanent damage such as fiber misalignment.

A carbon fiber reinforced composite with controllable stiffness could prove to be a suitable skin material in morphing

structures as it would offer high stiffness and yet flexibility when required.<sup>2</sup> In order to significantly deform conventional carbon fiber reinforced composites, high actuation forces are required that may cause the composite to fail before the required deformation has been achieved. The concept of a laminated carbon fiber reinforced material with controllable stiffness was also described previously.<sup>13–15</sup> A variable stiffness interleaved CFRP beam containing alternating layers of elastomer was developed by Raither et al.<sup>14</sup> The different fiber orientations of the reinforced layers permitted adaptive bend-twist coupling of the laminated composite when the elastomer was heated above its  $T_g$  (44 °C). The low  $T_g$  of the elastomer would limit the use of this composite in aerostructures where high operating temperatures are required. A disadvantage of interleaved composite designs is that there is a risk of delamination when the composite is deformed.

A diagram showing the concept of the controllable stiffness composite described in this study is shown in Figure 1. A

Received: June 26, 2013

Accepted: August 26, 2013

Published: August 26, 2013

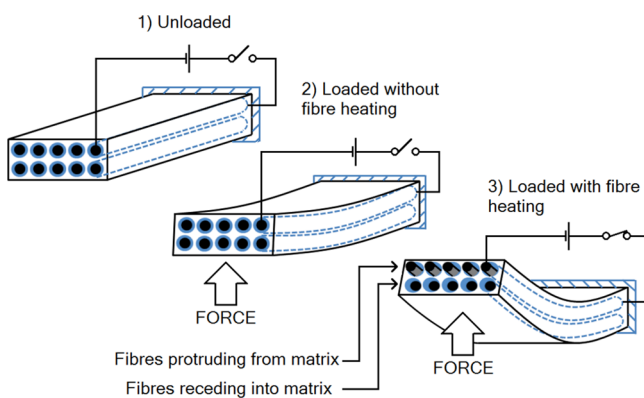


**Figure 1.** Concept of the controllable stiffness composite.

benefit of this concept is that the matrix remains stiff when the coating has softened. The composite can therefore withstand deformation at elevated temperature without the risk of misaligning the reinforcement. This form of coated-fiber composite also exhibits similar mechanical properties to those of uncoated carbon fiber reinforced composites, at temperatures lower than the softening temperature of the fiber coating. They are therefore suitable for high performance applications, and unlike interleaved composite designs there is no risk of delamination. Another advantage is that the thermoplastic coating can be heated quickly by passing a current through the carbon fibers, which allows stiffness control on demand.

Polyacrylamide was chosen as the fiber coating as it has a softening temperature of approximately 75 °C, when partially hydrated (20% moisture content), which is well below the  $T_g$  of the epoxy resin (182 °C) used as the matrix (Figure 5). The matrix resin can be either a thermoset or a thermoplastic as long as its  $T_g$  is above the softening temperature of the thermoplastic coating. There are a number of methods that can be used to covalently bond (graft) polymer coatings onto carbon fibers including electropolymerization or deposition,<sup>16,17</sup> plasma polymer deposition,<sup>18,19</sup> and in situ chemical grafting reactions.<sup>20,21</sup> For this study PAAm was electro-deposited (grafted) onto carbon fibers to provide good adhesion and to ensure suitable mechanical performance of the composite at room temperature. Good adhesion also ensures effective heat transfer between the fibers and the coating. Another advantage of using electrodeposition is that uniform layers of varying thickness can be coated onto the carbon fibers.<sup>17</sup>

## 2. EXPERIMENTAL SECTION

**2.1. Materials.** Unsized carbon fibers (AS4 12k HexTow) were kindly supplied by Hexcel Corporation (Duxford, Cambridge, UK). The aerospace grade resin system Araldite LY556 and hardener XB3473 was purchased from Huntsman Advanced Materials Ltd. (Cambridge, UK). A resin to hardener mixing ratio of 100:23 by mass was used as suggested by the manufacturers. Acrylamide (AAM) ( $\geq 99.5\%$  purity) and lithium perchlorate ( $\text{LiClO}_4$ ) were purchased from Sigma Aldrich (Dorset, UK) and used as received. Dimethylformamide (DMF) was purchased from VWR (UK), and n-dodecane (99%) was purchased from Fisher Scientific (UK).

**2.2. Preparation of PAAm Coated Carbon Fibers.** PAAm was electro-deposited onto unsized carbon fibers (AS4, Hexcel) continuously at 1.9 mm/s and under a constant tension of 150 g. The carbon fibers, acting as cathode, were electrically contacted by passing them over stainless steel pins connected to the negative terminal of a power supply (Statron YP 3218, 75 V and 4 A max, GDR) maintained at 1.2

A. The fibers were passed through a stainless steel tube connected to the positive terminal of the power supply. The fibers and stainless steel tube were immersed into 600 mL of electrolyte consisting of acrylamide (1.5 mol/dm<sup>3</sup>) dissolved in DMF (solvent) containing lithium perchlorate (0.25 mol/dm<sup>3</sup>). The bath was maintained at 65 °C. Polymer formation in the solution was not observed. The PAAm coated carbon fibers were washed thoroughly with acetone and deionized water followed by drying in an oven at 55 °C for 12 h.

**2.3. Characterization of Unsized and PAAm Coated Carbon Fibers.** All fiber specimens were conditioned for 10 days at 20 °C and at 80% relative humidity prior to characterization to ensure the PAAm coating was hydrated.

**Fiber Morphology.** The fibers were investigated using scanning electron microscopy (Hitachi S-3400N Variable Pressure SEM, Hitachi High Technologies America) at an accelerating voltage of 7 kV. Silver-loaded electrically conductive paint (RS, UK) was applied to one end of the specimen and the SEM stub to prevent charging.

**Fiber Diameters and Wettability.** The diameters of the carbon fibers were determined gravimetrically using the modified Wilhelmy-technique and calculated using eq 1

$$d_f = \frac{mg}{n\pi \cos \theta \gamma_{lv}} \quad (1)$$

where  $d_f$  is the fiber diameter,  $n$  is the number of fibers attached to the carrier ( $S$ ),  $m$  is the mass difference after emersion and immersion of carbon fibers in n-dodecane (recorded using a 4504 MP8 Sartorius ultramicrobalance, Göttingen, Germany),  $\theta$  is the contact angle (in this case zero), and  $\gamma_{lv}$  the surface tension of n-dodecane (25.4 mN/m). All measurements were taken in an air-conditioned room at 18 °C. The advancing and receding contact angles of five fibers immersed in deionized water ( $\gamma_{lv} = 72.8$  mN/m) were calculated using a rearrangement of eq 1:

$$\cos \theta = \frac{mg}{n\pi d_f \gamma_{lv}} \quad (2)$$

**Fiber Surface Composition.** The surface chemistry of the carbon fibers was analyzed using XPS on a Thermo VG Scientific Sigma Probe spectrometer equipped with an Al  $K_{\alpha}$  X-ray source ( $h\nu = 1468.6$  eV; power: 140 W). For the high-resolution spectra, the pass energy was set to 50 eV. An electron gun was used for charge compensation. Advantage v4.53 software was used to analyze the spectra.

**Thermal Analysis of Coating.** To quantify the amount of electrocoating on the carbon fibers TGA (TGA Q500, TA Instruments, USA) was used. The measurements were performed in air (60 mL/min) from 30 to 800 °C at a heating rate of 5 °C/min.

**Moisture Content of Coating.** Dynamic Vapor Sorption (DVS Advantage, SMS, UK) was used to determine the moisture content of the coated and unsized fibers. The samples were dried for 24 h at 40 °C and 0% relative humidity.

**Fiber Matrix Adhesion.** Single fiber pull out (SFPO) tests were used to quantify the interfacial shear strength ( $\tau_{\text{IFSS}}$ ), a measure of practical adhesion, between the carbon fibers (unmodified and coated) and an epoxy resin matrix (Araldite LY 556/Hardener XB 3473). The carbon fibers were embedded in the epoxy/hardener mixture to a length of 30–60  $\mu\text{m}$  using a custom built embedding apparatus. The epoxy was then cured at 160 °C for 12 h. A piezo-motor was used to pull the fiber out of the matrix at a speed of 0.2  $\mu\text{m/s}$ . The force was recorded by a load cell and logged using a computer. The interfacial shear strength ( $\tau_{\text{IFSS}}$ ) was calculated using eq 3

$$\tau_{\text{IFSS}} = \frac{F_{\text{max}}}{\pi d_f L} \quad (3)$$

where  $d_f$  is the fiber diameter,  $F_{\text{max}}$  is the maximum pull-out force, and  $L$  is the embedded length. The average interfacial shear strength was calculated from at least eight measurements.

**2.4. Fabrication of Pure Epoxy Samples and Carbon Fiber Reinforced Composites.** To fabricate pure epoxy specimens, the resin system (LY556/XB3473) was poured into a release fabric (FF03PM, Aerovac, West Yorkshire, UK) covered stainless steel mold

(80 mm × 50 mm × 2 mm). The resin was then cured inside a vacuum oven at 120 °C for 2 h and 180 °C for 4 h. The cured samples were then cut in 40 mm × 5 mm × 2 mm DMTA specimens using a diamond bladed cutter (Diadisc 4200, Mutronic, Rieden, Germany).

To manufacture prepreps, the unsized and PAAm coated fibers were wound at a constant tension (150 g force) onto a release fabric (FF03PM, Aerovac, West Yorkshire, UK) covered stainless steel plate (150 mm × 80 mm × 1 mm) using a filament winder (Kolelectric, Middlesex, UK). Two layers of fibers were wound onto the plate at 40 rpm. Epoxy resin (LY556/XB3473, Huntsman Advanced Materials Ltd., Cambridge, UK) was initially brushed by hand onto each fiber layer. This ensured complete infusion of the resin during the laminate fabrication. Resin Infusion under Flexible Tooling (RIFT) was then used to infuse, consolidate, and cure the laminates. The aim was to manufacture composites with fiber volume fractions of approximately 50%. The precoated fiber preform was placed on a heating plate (Wenesco, Inc., USA). The infusion procedure started with an air removal step, and then the fibers were left under vacuum ( $10^5$  Pa) for 20 min. The epoxy resin was heated to 40 °C and allowed to flow and infuse into the prepregged fiber laminate. The resin flow was stopped after it completely penetrated through the whole fiber layup. The fiber laminates were cured at 120 °C for 2 h and 180 °C for 4 h. The cured composites were cut into the required shape for the flexural tests (40 mm × 10 mm) and for DMTA (40 mm × 5 mm) using a diamond bladed cutter (Diadisc 4200, Mutronic, Rieden, Germany). The thickness of the composites was approximately 1.1 mm.

**2.5. Characterization of Pure Epoxy Resin and Carbon Fiber Reinforced Composites.** Prior to characterization, the pure epoxy samples and composite specimens were conditioned. Samples were either dried in a vacuum oven at 80 °C for 12 h, conditioned for 10 days at 20 °C and at 80% relative humidity, or fully submerged into water for 36 h. This allowed the effect of moisture content of the PAAm interphase on its glass transition temperature  $T_g$  to be studied. For this investigation the specimens are known as 'dry', hydrated, and 'fully hydrated', depending on the degree of conditioning. The weight before and after conditioning was measured using a microbalance. The volume fraction of carbon fibers within the composites was determined using acid digestion following procedure B described in ASTM D3171.

**Viscoelastic Properties.** The composites were analyzed using DMTA (Tritec 2000, Triton Technology Ltd., Keyworth, UK) in three point bending, at a heating rate of 5 °C/min, at 1 Hz, and at 0.05% strain. Single tests were performed for each sample except when stated otherwise. A hydrated PAAm coated fiber reinforced composite (conditioned for 10 days at 20 °C and at 80% relative humidity) was tested 5 times, from 30 °C to 140 °C, at the conditions stated above to determine how its properties changed after multiple heating cycles.

**Flexural Properties.** Three point bending tests were conducted in accordance with ASTM D7264 using an Instron 4505 (Bucks, UK) equipped with a 1 kN load cell. A span to thickness ratio of 32:1 was used. To determine the change in flexural modulus of a sample at elevated temperatures, each sample was firstly deflected at room temperature. The specimen was loaded to a maximum deflection of 0.5 mm to prevent failure and then unloaded. The test was then repeated at 110 °C and 130 °C and then again at room temperature. The specimens were heated with either an environmental chamber (SFL, Eurotherm, West Sussex, UK) or by applying a direct current (Votcraft DC power supply, max 30 V and 1.2 A, Berlin, Germany). Furthermore, composites were also tested to failure at room temperature to determine the flexural strength. For each condition at least six samples were tested.

### 3. RESULTS AND DISCUSSION

Composites consisting of unidirectional PAAm coated carbon fibers within an epoxy resin were manufactured. Heating the PAAm coating above its softening temperature was expected to dramatically reduce the flexural stiffness of the composite. Here we discuss the characterization of PAAm coated carbon fibers and the analysis of PAAm coated fiber reinforced composites at room and elevated temperatures.

**3.1. Quantity of PAAm Coating, Fiber Morphology, and Wettability.** As determined by TGA, 4 wt.% PAAm coating was successfully deposited onto the carbon fibers. Fiber diameters and wettability were determined gravimetrically using the modified Wilhelmy-technique (Table 1). The diameter of

**Table 1. Fiber Diameters and Contact Angles of Carbon Fibers in Water**

carbon fibers	fiber diameter/ $\mu\text{m}$	water contact angle/deg		
		$\theta_a$	$\theta_r$	$\Delta\theta$
unsized	$7.3 \pm 0.1$	$76 \pm 3$	$44 \pm 5$	32
PAAm coated	$7.5 \pm 0.1$	$34 \pm 5$	$29 \pm 3$	5

the unsized carbon fibers was  $7.3 \pm 0.1 \mu\text{m}$ . The diameter of the PAAm coated fibers increased to  $7.5 \pm 0.1 \mu\text{m}$ . This is consistent with the weight increase from TGA and shows the presence of a thin fiber coating. The unsized and PAAm coated carbon fibers had advancing contact angles in water ( $\theta_a$ ) of  $76 \pm 3^\circ$  and  $34 \pm 5^\circ$ , respectively. The unsized fibers are therefore more hydrophobic than the PAAm coated fibers. Contact angle hysteresis ( $\Delta\theta$ ) was calculated from the difference in the advancing and receding contact angles ( $\theta_r$ ). The  $\Delta\theta$  for the unsized and PAAm coated carbon fibers was 32 and 5, respectively. The smaller  $\Delta\theta$  for the PAAm coated fibers indicates chemical heterogeneity.<sup>2</sup> Scanning Electron Microscopy (SEM) was used to analyze the fiber morphologies (Figure 2). The surface of the clean, unsized fibers was smooth. A uniform coating was seen on the electrocoated carbon fibers. The coating had a droplet-chain like appearance and also had many small particulates adhering to the surface, which could be impurities within the polymer.

**3.2. Moisture Content and Chemical Composition of PAAm Coated Fibers.** Dynamic Vapor Sorption (DVS) was used to analyze the moisture content of the hydrated PAAm fiber coating. The unsized and PAAm coated fibers lost 0.03 wt.% and 0.8 wt.% moisture, respectively, when dried for 24 h. The moisture content of the PAAm coating was therefore calculated to be 19.3%. X-ray photoelectron spectroscopy (XPS) was used to analyze the surface composition of the original industrially oxidized and PAAm coated carbon fibers. The atomic composition of the unsized fibers, from the wide scan spectrum, was 87% carbon, 10% oxygen, and 3% nitrogen. The O:C ratio was 0.11. The composition of the PAAm coated fibers was 55% carbon, 30% oxygen, and 11% nitrogen. The O:C ratio for the coated fibers was 0.55. Pure PAAm should contain 60% carbon, 20% oxygen, and 20% nitrogen (O:C ratio of 0.33). The difference between the predicted composition and the measured values could be attributed to impurities within the monomer.<sup>22</sup> The higher percentage of oxygen in the coated fibers compared to the theoretical composition of PAAm could also be associated with moisture present in the PAAm coating. The deconvoluted high-resolution C 1s XP spectra confirm the presence of PAAm on the surface of the electrocoated fibers (Figure 2). For the unsized carbon fibers the C1s peak could be deconvoluted into four peaks at 285 eV (CHx), 286.3 eV (CN/C–O–C), 287.1 eV (C=O), and 289.3 eV (COOH),<sup>23,24</sup> two of which were also present in the PAAm coated fibers: 285 eV (CHx) and 286.3 eV (CN). However, an additional peak at 288.5 eV corresponding to the N–C=O bond present in polyacrylamide was also observed for the coated fibers.<sup>24,25</sup>

**3.3. Fiber/Matrix Adhesion.** The adhesion of the unsized and PAAm coated carbon fibers to an epoxy matrix was



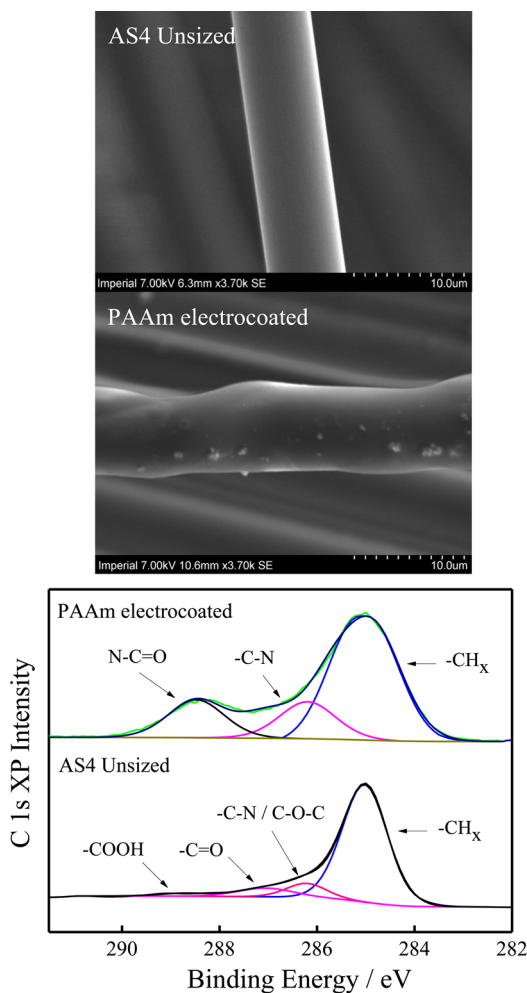


**Figure 2.** SEM images (top) and high resolution C 1s XP spectra (bottom) of AS4 unsized and PAAm electrocoated carbon fibers.

characterized using single fiber pull-out tests.  $\tau_{\text{IFSS}}$  of the unsized and PAAm coated fibers was  $101.2 \pm 2.6$  MPa and  $94.2 \pm 3.5$  MPa, respectively. The similarity of these results suggested the adhesion of the PAAm interphase to the carbon fibers and epoxy matrix was good. Representative force–displacement curves from SFPO tests are shown in Figure 3. The pull-out force initially increased linearly (point a) due to elastic deformation of the fiber/matrix interface. In some cases there was a decrease in the gradient of the force–displacement

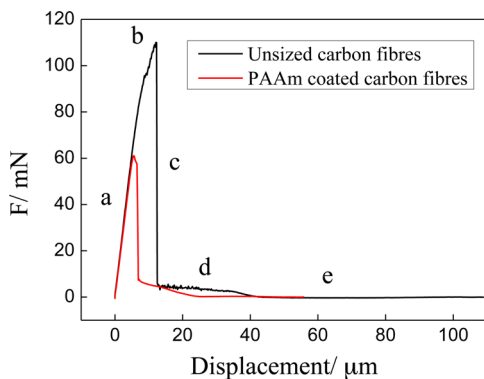


**Figure 3.** Fiber pull-out force–displacement curves of unsized and PAAm coated carbon fibers embedded in an epoxy matrix.

curve prior to the maximum force ( $F_{\text{max}}$ ). This could be due to yielding of the polymer at the interface or the initiation of debonding. At  $F_{\text{max}}$  (point b) the fiber/matrix interface failed suddenly, and the pull-out force dropped significantly (point c). The resistance to pull-out was now caused by friction between the debonded fiber and matrix (point d).<sup>26</sup> The force slowly decreased due to a reduction in contact area between the fiber and the matrix. At point 'e' the fiber was completely pulled out of the matrix. The displacement at which the force drops to zero represents the embedded fiber length ( $L$ ). The embedded lengths for the unsized and PAAm coated fibers were  $39 \pm 7$   $\mu\text{m}$  and  $35 \pm 15$   $\mu\text{m}$ , respectively. A higher  $F_{\text{max}}$  does not necessarily equate to a better adhesion between fiber and matrix as the  $\tau_{\text{IFSS}}$  depends on the embedded fiber length.<sup>27</sup>

The relationship of apparent interfacial shear strength as a function of the embedded fiber length between the unsized and electrocoated fibers and the epoxy matrix is shown in Figure 4.

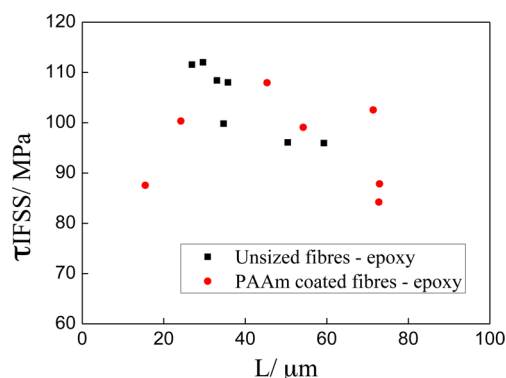


**Figure 4.** Interfacial shear strength ( $\tau_{\text{IFSS}}$ ) of unsized and PAAm coated carbon fibers as a function of the embedded fiber length ( $L$ ).

It has been reported that this relationship allows an interpretation of the fracture behavior between the fiber and the matrix.<sup>28</sup> The fiber/matrix boundary will have a ductile failure if an amorphous interphase is present. This leads to a plastic deformation at the boundary. On the other hand, the fiber–matrix fracture will exhibit brittle behavior if the interface fails immediately, which can be caused by crystalline structures at the interface or a highly cross-linked brittle epoxy resin. The failure between the fiber and matrix is classified as brittle if  $\tau_{\text{IFSS}}$  decreases with increasing embedded fiber length.<sup>29</sup> This behavior was observed for the unsized carbon fibers, whereas  $\tau_{\text{IFSS}}$  remained approximately constant with increasing embedded fiber length for the PAAm coated fibers, indicating a ductile failure. The amorphous PAAm coating therefore changed the interfacial failure mode by allowing some yielding before the interface completely failed.

**3.4. Viscoelastic Properties of Epoxy Matrix.** Dry and hydrated epoxy samples were analyzed using Dynamic Mechanical Thermal Analysis (Figure 5). The hydrated cured epoxy resin was conditioned for 10 days at 20 °C and at 80% relative humidity and the fully hydrated sample by submerging it into water for 36 h prior to analysis. The moisture content in the hydrated and fully hydrated sample was 0.7% and 0.8%, respectively. The  $T_g$ , taken as the peak temperature in the loss modulus (see Figure 5), of the dry epoxy sample was determined to be 199 °C. The  $T_g$  of the hydrated sample decreased to 193 °C due to the presence of water. The  $T_g$  of the fully hydrated sample was still lower at 187 °C. At 30 °C

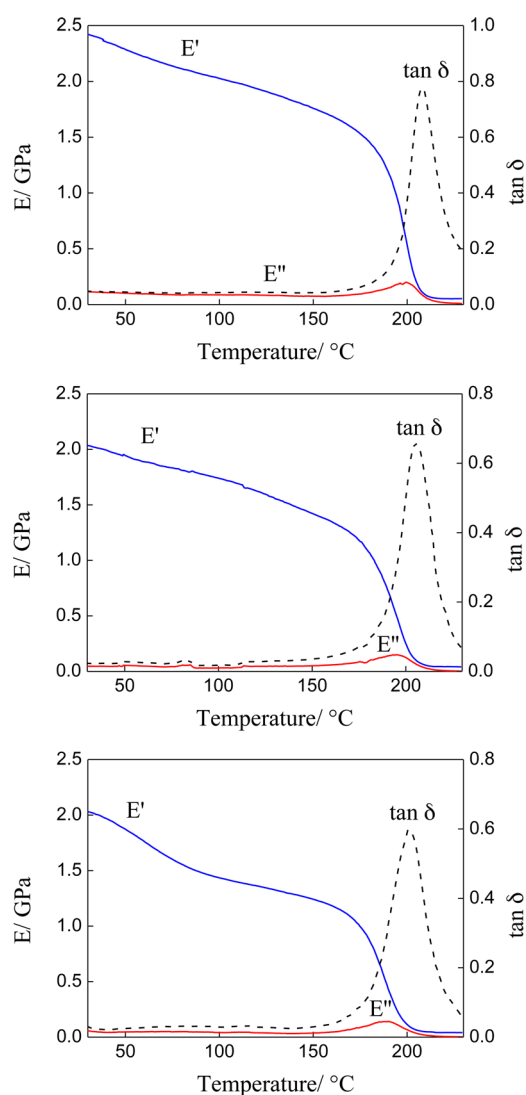


**Figure 5.** Storage modulus ( $E'$ ), loss modulus ( $E''$ ), and  $\tan \delta$  of the cured epoxy resin dry (top), the cured epoxy resin conditioned at 20 °C and 80% relative humidity (middle), and fully moisture saturated cured epoxy resin by water immersion (bottom) as a function of temperature.

the storage moduli of the dry, hydrated and fully hydrated samples were 2.43 GPa, 2.04 GPa, and 2.03 GPa, respectively. The storage modulus of all three samples dropped by >98% when heated to 230 °C. As each of the epoxy samples behaved similarly below the glass transition temperature, we can conclude that the contribution of the hydrated matrix in lowering the modulus of composites containing PAAm coated carbon fibers was insignificant.

**3.5. Fiber Volume Fraction, Void Content, and Viscoelastic Properties of Composites.** The fiber volume fractions of composites containing unsized and PAAm coated carbon fibers, determined following ASTM D 3171, were  $48 \pm 2\%$  and  $52 \pm 1\%$ , respectively. Acid digestion also revealed that relatively low void fractions (approximately 0.2%) were present in both composites. The viscoelastic properties of the composites containing unsized carbon fibers were determined using DMTA (Figure 6). At 30 °C the storage modulus of the dried composite was 82 GPa. The  $T_g$  of the epoxy was recorded to be 194 °C from the peak in the loss modulus (Figure 6). The moisture content in the hydrated and fully hydrated composites

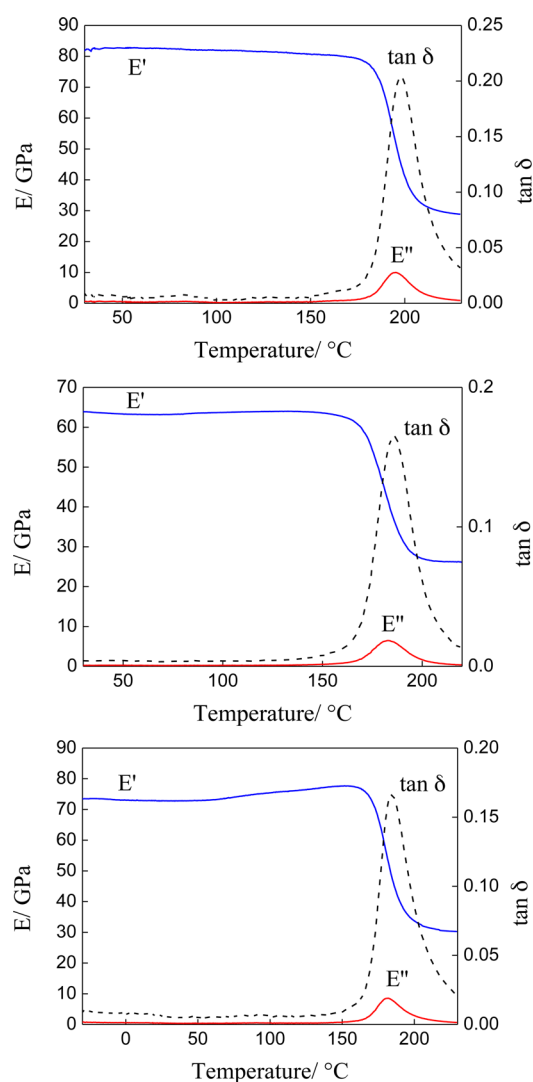


**Figure 6.** Storage modulus ( $E'$ ), loss modulus ( $E''$ ), and  $\tan \delta$  of a dried (top), hydrated (middle), and fully hydrated unsized carbon fiber reinforced epoxy composite (bottom) as a function of temperature.

containing unsized carbon fibers 0.3% and 0.6%, respectively. The hydrated unsized fiber reinforced composite (conditioned for 10 days at 20 °C and at 80% relative humidity) has a single  $T_g$  at 182 °C, corresponding to the epoxy resin. Below this temperature the storage modulus remained at approximately 63 GPa. The overall loss in stiffness from 30 °C to 230 °C was 59%. The  $T_g$  of epoxy in the fully moisture saturated unsized carbon fiber reinforced composite was measured to be 180 °C. The storage modulus of both hydrated samples increased at elevated temperature. This may be due to moisture evaporating from the composites.

Composites containing PAAm coated carbon fibers were also analyzed using DMTA (Figure 7). A PAAm coated fiber reinforced composite conditioned at 20 °C and 80% relative humidity was dried in a vacuum oven at 80 °C for 12 h. The  $T_g$  of the PAAm coating was 155 °C, which is close to the  $T_g$  of anhydrous PAAm (165 °C).<sup>30</sup> A 91% drop in storage modulus from 74 GPa to 7 GPa was recorded when the dried PAAm coated fiber reinforced epoxy composite was heated from 30 °C to 230 °C. This drop in stiffness was caused by the softening of both the dried PAAm and the epoxy. However, because of the

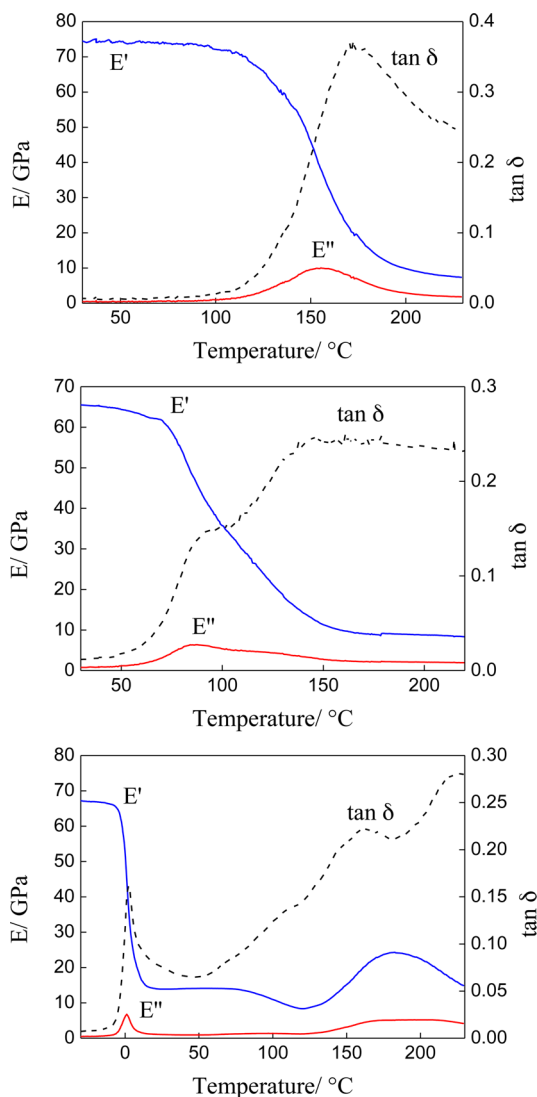


**Figure 7.** Storage modulus ( $E'$ ), loss modulus ( $E''$ ), and  $\tan \delta$  of a dried (top), hydrated (middle), and fully hydrated PAAm coated carbon fiber reinforced epoxy composite (bottom) as a function of temperature.

close proximity of the PAAm and epoxy glass transition temperatures it is difficult to discern the effect of the coating on the stiffness loss alone. The moisture content in the hydrated PAAm coated fiber reinforced composite (conditioned for 10 days at 20 °C and at 80% relative humidity) was 1.3%. At 30 °C the storage modulus of the composite was 66 GPa. At 130 °C the storage modulus dropped by 71% to 19 GPa. The PAAm coating within the composite exhibited a broad  $T_g$  around 84 °C that can be attributed to plasticization of the PAAm by adsorbed water in the partially hydrated polymer.<sup>31,32</sup> The overall loss in stiffness from 30 °C to 230 °C (including the contribution from the softened epoxy) was 88%. The  $T_g$  of the epoxy resin is only seen in the DMTA curves of the unsized fiber reinforced composite. This is because the storage modulus of this composite at its  $T_g$  (42 GPa at 182 °C) is higher than the  $E'$  of both PAAm coated fiber reinforced composites at this temperature. The composites containing hydrated and dried PAAm coated fibers had therefore softened to an extent where the epoxy  $T_g$  could no longer be detected. A sample of a composite containing PAAm coated carbon fibers was

submerged into water for 36 h. The moisture content in this fully hydrated composite was 10.7%. The  $T_g$  of the PAAm coating had dropped significantly to 1 °C due to moisture uptake. At -30 °C the storage modulus of the composite containing PAAm coated carbon fibers was 67 GPa. When this composite was heated through the  $T_g$  of the PAAm coating, from -30 °C to 30 °C, the storage modulus of the composite dropped by 79% to 14 GPa. A similar value (71%) was observed for the composite containing the partially hydrated PAAm coated fibers that was conditioned for 10 days at 20 °C and at 80% relative humidity. Therefore, hydrating the PAAm coating around the carbon fibers in the composites allowed to adjust the  $T_g$  of PAAm, which in turn enabled to reduce the composite stiffness at temperatures well below the  $T_g$  of the epoxy resin. The storage modulus of the fully moisture saturated composite containing PAAm coated fibers increased at temperatures exceeding 130 °C due to moisture evaporating from the composites. The  $T_g$  of epoxy in the fully saturated unsized fiber reinforced composite was recorded at 180 °C. For the fully hydrated PAAm coated fiber reinforced composite, the  $T_g$  of the epoxy matrix was very broad centered but around 187 °C. This is due to the combined drying of PAAm and epoxy.

Five heating/cooling cycles from 30 °C to 140 °C were performed on a composite containing partially hydrated PAAm coated carbon fibers using DMTA. No loss in performance was observed over the 5 cycles (Figure 8). This indicates that none of the constituents degraded and that the moisture content must have remained constant in the PAAm coating.

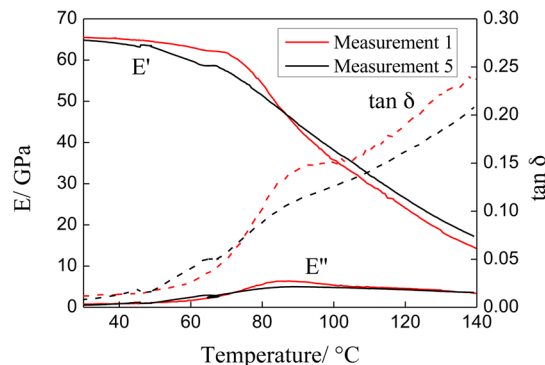


**Figure 8.** DMTA curves of hydrated PAAm coated fiber reinforced epoxy composite subjected to 1 and 5 heating cycles.

**3.6. Flexural Properties of Composites.** Three point bending tests were performed at room temperature, 110 °C, and 130 °C to determine the difference in composite stiffness at these temperatures. To prevent plastic deformation the hydrated composites (conditioned at 20 °C at 80% relative humidity) were deflected to 0.5 mm at each temperature. Load-displacement curves of the composites tested at different temperatures are shown in Figure 9. The gradient of the load-displacement curves remained unchanged when the hydrated composites containing unsized carbon fibers were heated in an environmental chamber. This was expected as the testing temperatures were below the  $T_g$  of the epoxy. However, the gradient of the slope decreased at elevated temperature when the composites were heated by applying a direct current to the carbon fibers. A possible explanation is that the actual temperature around the carbon fibers was significantly higher than temperature on the outer surface of the composites, where the temperature was recorded. The gradient of the load-

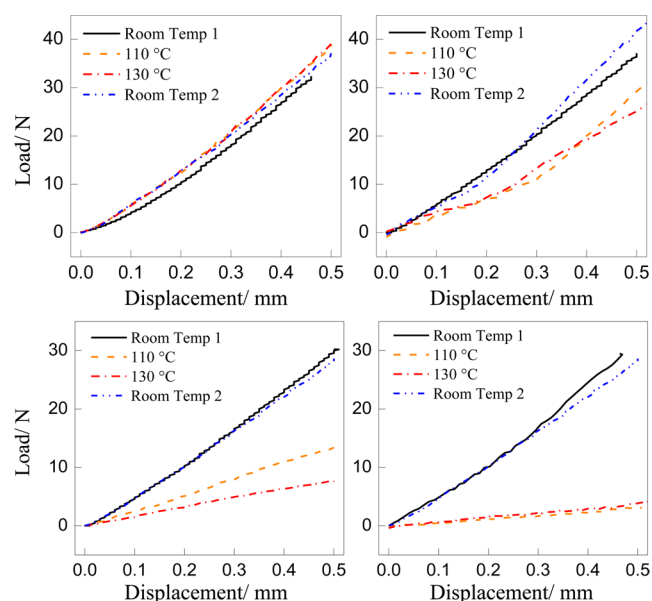


**Figure 9.** Representative load–displacement curves of unsized (top) and hydrated PAAm coated carbon fiber reinforced epoxy composites (bottom) at room temperature, 110 °C and 130 °C [composites heated using an environmental chamber (left) and an applied current (right)].

displacement curves for the hydrated PAAm coated fiber reinforced composites decreased significantly when the specimens were heated to 110 °C and 130 °C in an environmental chamber. The loss in stiffness was expected as the hydrated PAAm coating had been heated above its  $T_g$ . As with the unsized fiber reinforced composites, the gradient of the slope decreased when the specimens were heated using an applied current.

At room temperature the flexural stiffness of the unsized carbon fiber–epoxy composites was  $62 \pm 7$  GPa. No significant change in stiffness occurred when the unsized carbon fiber–epoxy composites were heated to 130 °C in an environmental chamber (Table 2). This behavior was expected as the testing temperatures were well below the  $T_g$  of the epoxy matrix. The composites were also heated to elevated temperatures during flexural tests by applying a direct current to the carbon fibers. Approximately 15 V and 0.6 A (9 W) were required to heat the entire flexural specimen (40 mm  $\times$  10 mm) to 110 °C and 20 V and 0.7 A (14 W) to heat the composites to 130 °C using a DC power supply. Again no significant change in stiffness was observed at these temperatures. At room temperature the flexural modulus of the conditioned composites containing

hydrated PAAm electrocoated carbon fibers ( $69 \pm 8$  GPa) remains similar to that of the unsized carbon fiber–epoxy composite. When tested at 110 °C and 130 °C in an environmental chamber, the flexural stiffness of the composites containing PAAm coated fibers dropped by 46% and 78%, respectively. A small 6% loss in stiffness was observed when the specimens were retested at room temperature, but this is not significant in view of the experimental scatter. Flexural tests were also performed at elevated temperature by passing a current through the carbon fibers. These tests were carried out to determine whether it was possible to heat the PAAm interphase without an external heating source. The same voltages and currents were applied to heat the PAAm coated fiber reinforced composites to 110 °C and 130 °C as for the unsized carbon fiber reinforced epoxy composites. When heated to 110 °C and 130 °C, the flexural modulus of the composite dropped to  $8 \pm 5$  GPa (88% reduction) and  $10 \pm 5$  GPa (86% reduction), respectively. The reductions in bending stiffness were higher when the composites were heated by passing a current through the carbon fibers rather than heating them in the environmental chamber. It is likely that the actual temperature around the carbon fibers was higher than the surface temperature of the composites. The reduction in stiffness was reversible; only a 4% loss in stiffness was recorded when retesting the composites at room temperature. This suggests that no permanent damage occurred by the heating and cooling cycles. It is also unlikely that there was significant thermal degradation of the PAAm coating as the thermal decomposition of polyacrylamide in nitrogen, which represents the environment of the fibers embedded in the composite, occurs above 350 °C.<sup>33</sup>

The unsized carbon fiber–epoxy composites had a flexural strength of  $420 \pm 25$  MPa. The flexural strength of the PAAm electrocoated carbon fiber–epoxy composites was  $136 \pm 21$  MPa. The poor flexural strength might be caused by the fact that many fibers were held together by the coating and were therefore not well impregnated with and distributed in the epoxy matrix. This could have been caused by poor spreading of the fibers during the coating process.

Tests were carried out to observe fibers sliding within the composite containing PAAm coated fibers at elevated temperature. To image the ends of the bent composites, to see whether the fibers were sliding, we had not only to cut but also to polish our composites, as the ends of the cut composites were too rugged to see any differences between straight and bent samples. Given a deflection of 1 mm at a span width of 32 mm we would expect a maximum displacement of the fibers of 30  $\mu$ m. The composites were deflected to 1 mm (in 3 point bending) at 130 °C within an environmental chamber. The

**Table 2.** Fiber Volume Fraction ( $V_f$ ), Void Content ( $V_v$ ), and Flexural Properties of Carbon Fiber Reinforced Epoxy Composites<sup>a</sup>

reinforcement	$V_f$ /%	$V_v$ /%	flexural modulus/GPa							flexural strength/MPa
			RT <sup>c</sup>	110 °C <sup>a</sup>	130 °C <sup>a</sup>	RT <sup>a,e</sup>	110 °C <sup>b</sup>	130 °C <sup>b</sup>	RT <sup>b,e</sup>	
unsized carbon fibers	$48 \pm 2$	$0.20 \pm 0.01$	$62 \pm 7$	$63 \pm 8$ (+2%)	$63 \pm 9$ (+2%)	$60 \pm 12$ (−3%)	$58 \pm 9$ (−6%)	$62 \pm 11$ (0%)	$60 \pm 8$ (−3%)	$420 \pm 25$
PAAm electrocoated carbon fibers <sup>c</sup>	$52 \pm 1$	$0.17 \pm 0.01$	$69 \pm 8$	$37 \pm 8$ (−46%)	$15 \pm 3$ (−78%)	$65 \pm 8$ (−6%)	$8 \pm 5$ (−88%)	$10 \pm 5$ (−86%)	$67 \pm 13$ (−3%)	$136 \pm 21$

<sup>a</sup>Specimens tested in an environmental chamber. <sup>b</sup>Specimens heated through an applied current and allowed to cool to RT. <sup>c</sup>Hydrated samples. <sup>d</sup>Figures in parentheses indicate changes of flexural modulus in percentages when compared to the initial room temperature values. <sup>e</sup>RT = room temperature.



specimens were then cooled in the deformed state. However, it was found that polishing “smeared” the composite surface, and so the fibers, PAAm coating, and matrix were indistinguishable and apparently fused, which constrained the fiber ends. Unfortunately, we observed no fiber sliding, but instead we observed the samples bent to a shape expected when the fiber ends were constrained (see the video in the Supporting Information). It is also likely that the PAAm coating had chemically bonded to the epoxy.<sup>34</sup> This would have limited the distance the fibers could slide within the composite. However, the video in the Supporting Information shows the behavior of a composite sample containing PAAm coated carbon fibers, which was bent in flexure at 130 °C to 1 mm, when heated unconstrained with a heat gun. It can be clearly seen that the bent composite straightens out and returns to its original shape.

However, in order to illustrate that the fibers do slide in “composites” containing coated fibers above the  $T_g$  of the coating we have manufactured a PVDF ( $T_g = -40$  °C) coated copper wire reinforced epoxy model composite (see the Supporting Information). When the specimen was bent at room temperature the metal wires slid within the wire coating adhering to the resin matrix because of the weak coating/wire interface. Images of the specimen were taken before and after bending (Figure S1, left and right, respectively). Prior to bending the composite the ends of the wires are in alignment with the epoxy matrix. When composites were bent by hand, the wires on the compression side of the composite can be seen protruding from the specimen. The wires on the tensile side are receding slightly, although this is not as obvious in these optical micrographs.

#### 4. CONCLUSIONS

In conclusion, it was demonstrated that thermosetting composites with controllable stiffness can be produced by applying a thermoplastic coating to carbon fibers with a  $T_g$  lower than that of the matrix. The flexural stiffness can be reduced and restored reversibly on demand by applying a direct current to the carbon fibers in order to heat a thin polyacrylamide interphase above its softening temperature. When this interphase softened, the fibers could move within the matrix, and, as a consequence, the flexural stiffness was significantly reduced. Therefore, these composites could be used in morphing applications where a stiff skin material is required that can be easily deformed on demand. For this proof-of-concept study PAAm was chosen as the thermoresponsive interphase as the  $T_g$  can be adjusted by controlling the hydration level of the polymer coating surrounding the fibers. Other polymers with softening temperatures above room temperature and below the  $T_g$  of the matrix could also be used. Composites containing PAAm electrocoated carbon fibers exhibited up to 88% reduction in flexural modulus when heated to 110 °C by passing a current through the fibers. The stiffness was recovered to the original value once the composites cooled to room temperature.

#### ■ ASSOCIATED CONTENT

##### Supporting Information

Video, text, and Figure S1. This material is available free of charge via the Internet at <http://pubs.acs.org>.

#### ■ AUTHOR INFORMATION

##### Corresponding Author

\*E-mail: [a.bismarck@imperial.ac.uk](mailto:a.bismarck@imperial.ac.uk), [alexander.bismarck@univie.ac.at](mailto:alexander.bismarck@univie.ac.at).

##### Notes

The authors declare no competing financial interest.

#### ■ ACKNOWLEDGMENTS

We acknowledge the Royal Thai government for providing a scholarship for C.T. and the UK Engineering and Physical Science Research Council (EPSRC) and MBDA for the CASE award for H.A.M.

#### ■ REFERENCES

- (1) James, T.; Menner, A.; Bismarck, A.; Iannucci, L. Morphing Skins: Development of New Hybrid Materials. *Proceedings of the 4th SEAS DTC Technical Conference*, Edinburgh, UK, July 7–8, 2009.
- (2) Tridech, C. Smart Fibre Coatings: Stiffness Control in Composite Structures. Ph.D. Thesis, Imperial College London, December 2011.
- (3) Thill, C.; Etches, J.; Bond, I.; Potter, K.; Weaver, P. J. *Aeronaut. J.* **2008**, *112*, 117–139.
- (4) Sofla, A. Y. N.; Meguid, S. A.; Tan, K. T.; Yeo, W. K. *Mater. Des.* **2010**, *31*, 1284–1292.
- (5) Henry, C.; McKnight, G. Deformable Variable-Stiffness Cellular Structures. U.S. Patent 7,678,440 B1, March 16, 2010.
- (6) Kornbluh, R. D.; Prahlad, H.; Pelrine, R.; Stanford, S.; Rosenthal, M. A.; von Guggenberg, P. A. Rubber to Rigid, Clamped to Undamped: Toward Composite Materials with Wide-Range Controllable Stiffness and Damping. *Proceedings of SPIE 5388, Smart Structures and Materials 2004: Industrial and Commercial Applications of Smart Structures Technologies*, San Diego, CA, March 14, 2004.
- (7) Peel, L. D.; Mejia, J.; Narvaez, B.; Thompson, K.; Lingala, M. J. *Mech. Des.* **2009**, *131*, 091003.
- (8) Kikuta, M. T. Mechanical Properties of Candidate Materials for Morphing Wings. M.S. Thesis, Virginia Polytechnic Institute and State University, December 2003.
- (9) Gandhi, F.; Kang, S. G. *Smart Mater. Struct.* **2007**, *16*, 1179–1184.
- (10) Murray, G.; Gandhi, F. *Smart Mater. Struct.* **2010**, *19*, 045002.
- (11) Gandhi, F.; Murray, G.; Kang, S. G. *AIAA J.* **2009**, *47*, 757–766.
- (12) McKnight, G.; Henry, C. Variable Stiffness Materials for Reconfigurable Surface Applications. *Proceedings of SPIE 5761, Smart Structures and Materials 2005: Active Materials: Behavior and Mechanics*, San Diego, CA, March 6, 2005.
- (13) Bergamini, A.; Christen, R.; Motavalli, M. *Smart Mater. Struct.* **2007**, *16*, 575–582.
- (14) Raither, W.; Bergamini, A.; Gandhi, F.; Ermanni, P. *Composites, Part A* **2012**, *43*, 1709–1716.
- (15) McKnight, G.; Barvosa-Carter, W. Variable Stiffness Structure. U.S. Patent 7,892,630 B1, February 22, 2011.
- (16) Labronici, M.; Ishida, H. *Compos. Interfaces* **1994**, *2*, 199–234.
- (17) Bismarck, A.; Menner, A.; Kumru, M. E.; Sezai Sarac, A.; Bistriz, M.; Schulz, E. J. *Mater. Sci.* **2002**, *37*, 461–471.
- (18) Kettle, A. P.; Beck, A. J.; O’Toole, L.; Jones, F. R.; Short, R. D. *Compos. Sci. Technol.* **1997**, *52*, 1023–1032.
- (19) Kettle, A. P.; Jones, F. R.; Alexander, M. R.; Short, R. D.; Stollenwerk, M.; Zabold, J.; Michaeli, W.; Wu, W.; Jacobs, E.; Verpoest, I. *Composites, Part A* **1998**, *29*, 241–50.
- (20) Bismarck, A.; Pfaffernoschke, M.; Springer, J. J. *Appl. Polym. Sci.* **1999**, *71*, 1175–1185.
- (21) Koschinski, I.; Reichert, K.-H. *Makromol. Chem., Rapid Commun.* **1988**, *9*, 291–298.
- (22) Uchida, E.; Uyama, Y.; Iwata, H.; Ikada, Y. *J. Polym. Sci., Part A: Polym. Chem.* **1990**, *28*, 2837–2844.
- (23) Briggs, D. *Surface Analysis of Polymers by XPS and Static SIMS*; Cambridge University Press: Cambridge, 1998; p 48.



- (24) Beamson, G.; Briggs, D. *High Resolution XPS of Organic Polymers: The Scienta ESCA 300 Database*; Wiley: Chichester, 1992; p 295.
- (25) Lanniel, M.; Huq, E.; Allen, S.; Buttery, L.; Williams, P. M.; Alexander, M. R. *Soft Matter* **2011**, *7*, 6501–6514.
- (26) Hull, D.; Clyne, T. W. *An Introduction to Composite Materials*, 2nd ed.; Cambridge University Press: Cambridge, 1996; p 140.
- (27) Ho, K. K. C.; Lamoriniere, S.; Kalinka, G.; Schulz, E.; Bismarck, A. J. *Colloid Interface Sci.* **2007**, *313*, 476–484.
- (28) Ramanathan, T.; Bismarck, A.; Schulz, E. K.; Subramanian, K. *Compos. Sci. Technol.* **2001**, *61*, 1703–1710.
- (29) Meretz, S.; Auersch, W.; Marotzke, C.; Schulz, E.; Hampe, A. *Compos. Sci. Technol.* **1993**, *48*, 285–290.
- (30) Fox, R. B. Glass Transition Temperature of Selected Polymers. In *CRC Handbook of Chemistry and Physics*, 93rd ed.; Haynes, W. M., Ed.; CRC Press: US, 2012; pp 13–10.
- (31) Qutubuddin, S.; Lin, C. S.; Tajuddin, Y. *Polymer* **1994**, *35*, 4606–4610.
- (32) Yuen, H. K.; Tam, E. P.; Bullock, J. W. On the Glass Transition Temperature of Polyacrylamide. In *Analytical Calorimetry*; Johnson, J. F., Gill, P. S., Eds.; Springer: US, 1984; Vol. 5, pp 13–24.
- (33) Kitahara, Y.; Okuyama, K.; Ozawa, K.; Suga, T.; Takahashi, S.; Fujii, T. J. *Therm. Anal. Calorim.* **2012**, *110*, 423–429.
- (34) Zhang, M. Q.; Rong, M. Z.; Yu, S. L.; Wetzels, B.; Friedrich, K. *Wear* **2002**, *253*, 1086–1093.